Journal of Global Positioning Systems (2007)
Vol.6, No.1: 65-73

Modified Gaussian Sum Filtering Methods for INS/GPS Integration

Yukihiro Kubo, Takuya Sato and Sueo Sugimoto

Department of Electrical and Electronic Engineering, Ritsumeikan University, Shiga, Japan, 525-8577

Abstract. In INS (Inertial Navigation System) /GPS (Global Positioning System) integration, nonlinear models should be properly handled. The most popular and commonly used method is the Extended Kalman Filter (EKF) which approximates the nonlinear state and measurement equations using the first order Taylor series expansion. On the other hand, recently, some nonlinear filtering methods such as Gaussian Sum filter, particle filter and unscented Kalman filter have been applied to the integrated systems. In this paper, we propose a modified Gaussian Sum filtering method and apply it to land-vehicle INS/GPS integrated navigation as well as the in-motion alignment systems. The modification of Gaussian Sum filter is based on a combination of Gaussian Sum filter and so-called unscented transformation which is utilized in the unscented Kalman filter in order to improve the treatment of the nonlinearity in Gaussian Sum filter. In this paper, the performance of modified Gaussian Sum filter based integrated systems is compared with other filters in numerical simulations. From simulation results, it was found that the proposed filter can improve transient responses of the filter under large initial estimation errors.

Key words: INS , GPS, integration, nonlinear filter

1 Introduction

In the INS/GPS integrated system, the complementary characteristics of INS and GPS are exploited. INS provides position, velocity and attitude information at a high update rate with the continuous availability, and the long term accuracy of position and velocity information of GPS prevents the growing navigation errors of INS. In other words, the navigation errors of INS are estimated and corrected by using GPS measurements (Siouris, 1993; Grewal, 2001).

For many years, the extended Kalman filter (EKF) has been widely utilized as the estimator in the integrated navigation systems (Maybeck, 1979; Gelb, 1974). Additionally, in the case of conventional navigation systems, the initialization of INS navigation states is completed prior to vehicle motion and then the ordinary integrated navigation is implemented. Usually, this initialization method needs 5 to 10 minutes and the vehicle must be stopped. It is, however, inconvenient and impractical when there is not enough time to stop at a start point. Thus it is motivated to develop in-motion alignment and navigation algorithms which can provide the accurate attitude information while moving. Because the initial attitude of the land-vehicle is unknown, the attitude is usually assumed to be 0. Thus, when the initial heading error is large, the nonlinear character of the INS error equations is emphasized for in motion alignment (Rogers, 2001). Therefore several nonlinear filtering methods such as Monte Carlo filter (Kitagawa, 1996; Doucet, 2000), Quasi-linear optimal filter (Sunahara, 1970), Gaussian Sum filter (Alspach, 1972) and unscented Kalman filter (Julier, 2000), have been applied to the integrated navigation systems. The performance comparisons of the nonlinear filters in the integrated navigation systems also have been reported by the authors (Tanikawara, 2004; Fujioka, 2005; Nishiyama, 2006).

According to (Nishiyama, 2006), although Gaussian Sum filter (GSF) works well with large uncertainties in the initial attitude information, the linearization technique is employed similarly to the extended Kalman filter. On the other hand, the unscented Kalman filter (UKF) has been recently paid much attention in the area of the integrated navigation (Yi, 2005; An, 2005; Shin, 2007). The unscented Kalman filter calculates the predicting mean and covariance of the state vector from a set of samples that are called sigma points by means of so-called unscented transformation. In this paper, we try to combine the GSF and the unscented transformation in order to improve the treatment of the nonlinearity in the GSF. With this combination, it is expected that the transient response of the filter can be improved under large initial estimation errors.

In this paper, firstly we briefly review the algorithms of the nonlinear filters that are applied in this paper. Then, the modified Gaussian Sum filtering algorithm is derived by utilizing the unscented transformation. Finally, the performance of EKF, GSF, UKF based and modified Gaussian Sum filter based integrated systems is compared in numerical simulations.

2 Description of the system

In this work, closed-loop, tightly coupled mechanization is adopted for the INS/GPS integration. Fig. 1 shows the architecture of the integration with major data paths between the system components. The components of the system are strapdown INS and GPS receiver. The INS contains IMU (Inertial Measurement Unit: accelerometer and gyro). Based on the measured acceleration and angular rate, the INS computes the position, velocity and attitude of the vehicle relative to their initial value at high frequency. But there exist unbounded position errors that grow slowly with time. The concept of the integrated navigation system of Fig. 1 is to reduce the INS errors by using some external measurement from a GPS receiver. In this research, GPS double differenced carrier phase and undifferenced Doppler measurements are employed as external measurements to remove the INS errors. The nonlinear filter estimates the errors in the navigation and attitude information using the raw GPS data.

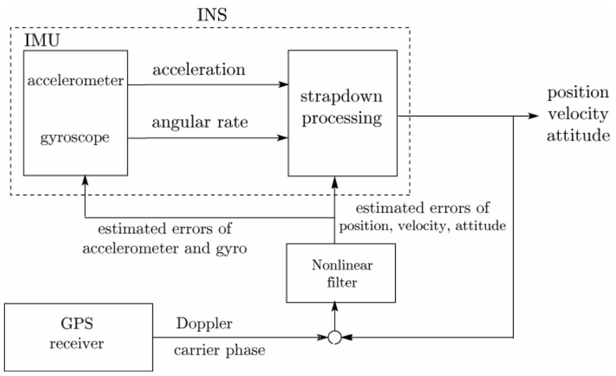

Fig. 1. Description of the system

2.1 Coordinate systems

To integrate the navigation systems, definitions of coordinate systems that the navigation systems or included sensors refer to are important. This section defines the coordinate frames used in this paper and represents the angular relationship between them. The coordinate frames are defined as follows:

1) The E frame (X_E, Y_E, Z_E) is the right-handed earth fixed coordinate frame. It has the origin at the center of the earth; the Z_E - axis is directed toward the North Pole; the X_E - and Y_E - axes are located in the equatorial plane, whereby the X_E - axis is directed toward the Greenwich Meridian. It is used for the definition of position location such as latitude and longitude.

2) The L frame (X_L, Y_L, Z_L) is the right-handed locally level coordinate frame. The X_L - and Y_L - axes are directed toward local north and east respectively; Z_L - axis is downward vertical at the local earth surface referenced position location. It is used for defining the angular orientation of the local vertical in the E frame.

3) The C frame (X_C, Y_C, Z_C) is the right-handed computer frame that is defined by rotating the L frame around negative Z_L - axis by the “wander angle” α ; toward the negative Y_L - axis and the Z_C - axis is directed toward the negative Z_L - axis (upward vertical). It is used for integrating acceleration into velocity, and used as the reference for describing the strapdown sensor coordinate frame orientation.

4) The B frame (X_B, Y_B, Z_B) is the strapdown inertial sensor coordinate frame (body frame). The X_B - axis is directed toward the head of the vehicle; the Y_B - axis is the right-hand of the vehicle; the Z_B - axis is downward vertical to the X_B - Y_B plane. The frame is fixed on the vehicle and rotates with the motion of the vehicle.

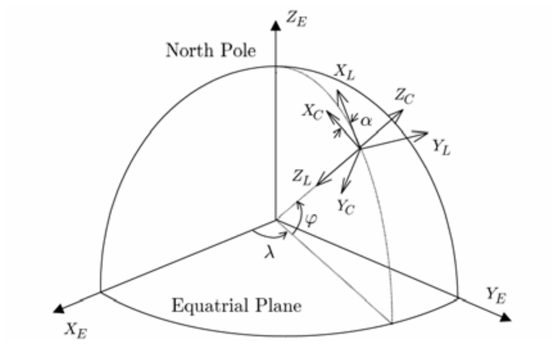

Fig. 2. Coordinate frames

Fig. 2 shows the spatial image of the *E*, *L* and *C* frames, where λ and φ represent the longitude and the latitude respectively. In the inertial computations, the acceleration sensed with respect to the *B* frame have to be transformed onto the *C* frame. The velocity and position of the vehicle are then computed with respect to the *C* frame. Such a transformation is known as the Euler angle transformation. We define the product of direction cosine matrix for this transformation as T_B^C . Then the coordinates (x_B, y_B, z_B) in the *B* frame are transformed into (x_C, y_C, z_C) in the *C* frame as follows:

$$\begin{bmatrix} x_C \\ y_C \\ z_C \end{bmatrix} = T_B^C \begin{bmatrix} x_B \\ y_B \\ z_B \end{bmatrix} \tag{1}$$

where T_B^C is the direction cosine matrix.

3 INS error model

The direction cosine matrix T_E^C is represents the transformation from the E frame to the C frame, and it can be decomposed as follows.

$$T_E^C = T_L^C T_E^L \tag{2}$$

On the other hand, the computed matrices $\overline{T_L^C}$ and $\overline{T_E^L}$ contain errors δT_L^C and δT_E^L respectively. The error δT_C^E can be formulated as

$$\begin{aligned} \delta T_E^C &\equiv \overline{T_E^C} - T_E^C \\ &= \overline{T_L^C}\,\overline{T_E^L} - T_L^C T_E^L \\ &= \{\delta T_L^C [I - (\delta r_L \times)] - T_L^C (\delta r_L \times)\} T_E^L \\ &= \mathcal{R} T_E^L \end{aligned} \tag{3}$$

where $\delta r_L \equiv [\,\delta r_{L,x}\,,\, \delta r_{L,y}\,,\, 0\,]^{\mathsf{T}}$ is horizontal angular position error, and the relation of $\overline{T_E^L} = [I - (\delta r_L \times)] T_E^L$ is used in the calculation of equation (3) with the assumption that $\delta r_{L,x}$ and $\delta r_{L,y}$ are small. Also, $(a\times)$ for 3×1 vector $a = [\,a_x\,, a_y\,, a_z\,]^{\mathsf{T}}$ is the skew- symmetric matrix defined by

$$(a\times) \equiv \begin{bmatrix} 0 & -a_z & a_y \\ a_z & 0 & -a_x \\ -a_y & a_x & 0 \end{bmatrix} \tag{4}$$

And $\mathcal{R}$ is the position error matrix defined as follows (Rogers 2003, 2001).

$$\mathcal{R} \equiv \begin{bmatrix} \delta\cos\alpha & -\delta\sin\alpha & \delta r_{C,y}\cos\delta\alpha - \delta r_{C,x}\sin\delta\alpha \\ -\delta\sin\alpha & -\delta\cos\alpha & -\delta r_{C,x}\cos\delta\alpha - \delta r_{C,y}\sin\delta\alpha \\ -\delta r_{L,y} & \delta r_{L,x} & 0 \end{bmatrix} \tag{5}$$

where

$$\delta\sin\alpha \equiv \sin(\alpha + \delta\alpha) - \sin\alpha \tag{6}$$

$$\delta\cos\alpha \equiv \cos(\alpha + \delta\alpha) - \cos\alpha \tag{7}$$

According to (Rogers, 2001, 2003), we have

$$\dot{\mathcal{R}} = \mathcal{R}(\omega_{E/L}^L \times) - (\overline{\omega_{E/C}^C} \times)(T_L^C + \mathcal{R}) + (\omega_{E/C}^C \times) T_L^C \tag{8}$$

where the dot above a letter denotes differentiation with respect to time, the vector $\omega_{E/L}^L$ is the rotation rate of the L frame with respect to the E frame in the L frame coordinate system, and the vector $\omega_{E/C}^C$ is similarly defined. From equation (8), the position error ($\delta r_{C,x}$, $\delta r_{C,y}$) as well as azimuth error ($\delta\alpha$) equations can be derived.

3.1 Velocity error model

The computed velocity $\overline{v_C}$ also contains the velocity error $\delta \boldsymbol{v}_C$ such that

$$\overline{v_C} = v_C + \delta v_C \tag{9}$$

and the velocity equation is given by

$$v_C = f_C - (\rho_C + 2\Omega_C) \times v_C + g_C \tag{10}$$

where f_C is non-gravitational specific force vector, ρ is relative rate vector, and Ω_C is earth rate vector. The specific force is proportional to the inertial acceleration of the system due to all forces except gravity measured by the accelerometer. g_C is the gravity vector, positive toward the centre of the earth in the C frame. From equations (9) and (10), the velocity error is modelled by

$$\begin{aligned} \delta\dot{v}_C &= b_C + f_C \times \delta\theta_C + v_C \times (\delta\rho_C + 2\delta\Omega_C) \\ &\quad - (\rho_C + 2\Omega_C) \times \delta v_C \\ &\quad - (\delta\rho_C + 2\delta\Omega_C) \times \delta v_C + \delta g_C \end{aligned} \tag{11}$$

where $\delta\theta_C \equiv [\,\delta\theta_{C,x}\,, \delta\theta_{C,y}\,, \delta\theta_{C,z}\,]^{\mathsf{T}}$ is the attitude error.

3.2 Attitude error model

The attitude error $\delta\theta_C$ causes the error of the transformation matrix T_B^C . The computed matrix $\overline{T_B^C}$ which contains the attitude error is formulated by

$$\overline{T_B^C} = [I - (\delta\theta_C \times)] T_B^C \tag{12}$$

Therefore, we have following attitude error model.

$$\delta\dot{\theta}_C = \delta\omega_{E/C}^C + \delta\omega_{I/E}^C + \delta\theta_C \times \omega_{I/C}^C + d_C \tag{13}$$

where d_C denotes gyro drift.

3.3 Sensor error model

In this paper, the accelerometer bias b_B and gyro bias d_B are modelled as the first order Markov processes respectively as follows:

$$\begin{aligned} \dot{b}_B(t) &= -\frac{1}{\tau_b} b_B(t) + u_b(t) \\ \dot{d}_B(t) &= -\frac{1}{\tau_d} d_B(t) + u_d(t) \end{aligned} \tag{14}$$

where τ_b and τ_d are the correlation time constants and $u_b(t)$, $u_d(t)$ are zero mean Gaussian white noise processes.

3.4 State equation

In order to implement the nonlinear filtering for integrated navigation, here, we define the state vector. Because the double differenced carrier phases are used as the measurements in this paper, the unknown integer ambiguities should be simultaneously estimated. Therefore the state vector is defined such that it includes the INS errors as well as the integer ambiguities as follows:

$$\begin{aligned} \boldsymbol{x} = \big[& \delta r_{C,x}, \delta r_{C,y}, \delta v_{C,x}, \delta v_{C,y}, \delta\theta_{C,x}, \delta\theta_{C,y}, \delta h_C, \\ & \delta v_{C,z}, b_{B,x}, b_{B,y}, b_{B,z}, d_{B,x}, d_{B,y}, d_{B,z}, \gamma, \beta, \\ & c\delta t, N_{k,u}^{1,2}, N_{k,u}^{1,3}, \ldots, N_{k,u}^{1,n_s} \big]^{\mathsf{T}} \end{aligned} \tag{15}$$

where $N_{k,u}^{1,2}$ denotes the double differenced integer ambiguity of the satellites 1, 2 and the receivers k, u, and n_s is the number of visible satellites. β and γ are defined as follows:

$$\beta \equiv \cos\delta\alpha - 1$$
$$\gamma \equiv \sin\delta\alpha$$

The descriptions of the state vector components are listed in Table 1. Then, from equations (8), (11), (13) and (14), the state equation can be formulated by

$$\dot{x}(t) = f(x(t), t) + \eta(t) \tag{16}$$

where $f(\bullet, t)$ is the time-varying nonlinear function, and the process noise $\eta(t)$ is assumed to be mutually independent zero mean Gaussian white noise with covariance matrix $N(t)$.

Table 1. List of states

No.	Symbol	Error state
1	$\delta r_{C,x}$	X_C -axis position error in angle
2	$\delta r_{C,y}$	Y_C -axis position error in angle
3	$\delta v_{C,x}$	X_C -axis velocity error
4	$\delta v_{C,y}$	Y_C -axis velocity error
5	$\delta\theta_{C,x}$	X_C -axis tilt error
6	$\delta\theta_{C,y}$	Y_C -axis tilt error
7	γ	$\sin\delta\alpha$
8	β	$\cos\delta\alpha - 1$
9	δh_C	Z_C -axis altitude error
10	$\delta v_{C,z}$	Z_C -axis velocity error
11	$b_{C,x}$	X_B -axis accelerometer bias
12	$b_{C,y}$	Y_B -axis accelerometer bias
13	$b_{C,z}$	Z_B -axis accelerometer bias
14	$d_{C,x}$	X_B -axis gyro bias
15	$d_{C,x}$	Y_B -axis gyro bias
16	$d_{C,x}$	Z_B -axis gyro bias,
17 ⋮	$N_{k,u}^{1,2}$ ⋮	double differenced ambiguity ⋮

By discretizing the state equation (16), we have

$$x(k+1) = x(k) + f(x(k), k)\Delta t + w(k) \tag{17}$$

where $w(k)$ is assumed to be Gaussian white noise with zero mean and diagonal covariance matrix $Q(k)$, and Δt is a sampling interval of the measurement data.

3.5 Measurement equation

In this paper, the measurements are the double differenced carrier phase and Doppler data. By ignoring some errors in the carrier phase data such as the remaining ionospheric and tropospheric delays and multipath errors, then the double differenced carrier phase measurement can be simply modelled by

$$y(k) = h(r_E) + \lambda N_{ku} + \varepsilon_g(k) \tag{18}$$

where r_E is the position vector in the E frame, the function h is the nonlinear function that indicates the distance between satellites and receivers, N_{ku} is the ambiguity vector, λ is the wave length, and ε_g is the measurement noise.

By linearlizing equation (18) with the first order Taylor series approximation around the position indicated by INS, $r_E^i(k)$, and applying appropriate transformations of the coordinate systems, we obtain the measurement equation of the INS position error in the C frame as follows.

$$\begin{aligned}\tilde{y}(k) &\equiv y(k) - h(r_E^i(k)) \\ &= \hat{H}(k)\delta r_C(k) + \lambda N_{ku} + \varepsilon_g(k)\end{aligned} \tag{19}$$

where

$$\hat{H}(k) \equiv -\tilde{H}(k)T_L^E(k)T_A(k)T_B(k)T_C^L(k) \tag{20}$$

and

$$\tilde{H}(k) \equiv \left[\frac{\partial h(r_E(k))}{\partial r_E(k)}\right]_{r_E(k)=r_E^i(k)},$$

$$T_A \equiv \begin{bmatrix} -(R_p+h) & 0 & 0 \\ 0 & \dfrac{R_p+h}{\cos\lambda} & 0 \\ 0 & 0 & 1 \end{bmatrix}, \quad T_B \equiv \begin{bmatrix} 0 & 1 & 0 \\ 1 & 0 & 0 \\ 0 & 0 & 1 \end{bmatrix}$$

where R_p is the earth radius.

The Doppler measurement can be modelled by the change of the distance between the receiver and the satellite in the sampling interval Δt (Misra, 2001). By using the velocity error vector in the C frame, $\delta \mathbf{v}_C$, and the appropriate transformations similarly to the above derivations, the Doppler measurement can be formulated as

$$D_u(k) = G_u(k)\left\{\tilde{T}_C^E(v_C^i - \delta v_C) - v_E^p\right\} + \mathbf{1}c\delta\dot{t}_u + \varepsilon_d(k) \tag{21}$$

where

$$G_u \equiv \left[g_u^{1\,\mathrm{T}}\ g_u^{2\,\mathrm{T}} \cdots g_u^{n_s\,\mathrm{T}}\right]^{\mathrm{T}}, g_u^p \equiv \left[\frac{\partial r_u^p}{\partial r_E}\right]_{r_E=r_E^i}^{\mathrm{T}},$$

$$\tilde{T}_C^E \equiv \left[(T_C^E)^{\mathrm{T}}\ (T_C^E)^{\mathrm{T}} \cdots (T_C^E)^{\mathrm{T}}\right]^{\mathrm{T}}$$

and r_u^p denotes the distance between the receiver u and the satellite p, v_E^p is the velocity of the satellite p in the E frame and ε_d is the measurement noise. Then, we have the following Doppler measurement equation.

$$\begin{aligned}\tilde{D}_u(k) &\equiv D_u + G_u v_E^p - G_u\tilde{T}_C^E v_c^i \\ &= \left[-G_u\tilde{T}_C^E \quad 1\right]\begin{bmatrix}\delta v_C \\ c\delta\dot{t}_u\end{bmatrix} + \varepsilon_d\end{aligned} \tag{22}$$

Finally, from equations (19) and (22), we have the measurement equation for the integrated navigation in general form:

$$z(k) = H(k)x(k) + \varepsilon(k) \tag{23}$$

where $z(k) \equiv [y^{\mathrm{T}}(k)\ \ \tilde{D}_u^{\mathrm{T}}(k)]^{\mathrm{T}}$.

4 Nonlinear filtering

Nonlinear filtering techniques are applied to the integrated INS/GPS system in order to estimate the state vector (the errors of INS described above). In this section, firstly, we briefly review the filter algorithms of the GSF and the UKF. Then the modified Gaussian Sum filter (MGSF) algorithm is derived.

4.1 Gaussian Sum filtering

Let Z_k be the set of the measurement such that

$$Z_k = \{z(1), z(1), \ldots, z(k)\} \tag{24}$$

In the GSF (Alspach, 1972), a posteriori probability density $p(x(k) \mid Z_k)$ is formed by the convex combination of the outputs of several Kalman filters processed in parallel. The a priori density $p(x(k) \mid Z_{k-1})$ is assumed that it is formulated by the sum of several normal distributions as follows:

$$\begin{aligned}p(x(k) \mid Z_{k-1}) &= \sum_{j=1}^{m} \gamma^j(k \mid k-1) \\ &\quad \times N\left[\mu^j(k \mid k-1), P_\mu^j(k \mid k-1)\right]\end{aligned} \tag{25}$$

where m is the number of distributions, and γ^j is the weight for the j-th distribution such that

$$\sum_{j=1}^{m} \gamma^j(k \mid k-1) = 1, \quad \gamma^j(k \mid k-1) \geq 0$$

And $N[\theta, \Sigma]$ denotes the normal probability density function with mean θ and covariance matrix Σ. Then, by the Bayesian recursion relations, a posteriori density can be formulated by

$$p(x(k) \mid Z_k) = \sum_{j=1}^{m} \gamma^j(k \mid k) N\left[\mu^j(k \mid k), P_\mu^j(k \mid k)\right] \tag{26}$$

where

$$\begin{aligned}\mu^j(k \mid k) &= \mu^j(k \mid k-1) \\ &\quad + K_\mu^j(k)\left(z(k) - H(k)\mu^j(k \mid k-1)\right)\end{aligned}$$

$$P_\mu^j(k \mid k) = P_\mu^j(k \mid k-1) - K_\mu^j(k)H(k)P_\mu^j(k \mid k-1)$$

$$\begin{aligned}K_\mu^j(k) &= P_\mu^j(k \mid k-1)H(k)^{\mathrm{T}} \\ &\quad \left[H(k)P_\mu^j(k \mid k-1)H(k)^{\mathrm{T}} + R(k)\right]^{-1}\end{aligned}$$

and the weight $\gamma^j(k \mid k)$ is given by

$$\gamma^j(k \mid k) = \frac{\gamma^j(k \mid k-1)\beta^j(k)}{\sum_{l=1}^{m}\{\gamma^l(k \mid k-1)\beta^l(k)\}} \tag{27}$$

where

$$\gamma^j(k\,|\,k-1) = \gamma^j(k-1\,|\,k-1)$$
$$\beta^j(k) = N\left[\nu^j(k\,|\,k-1), P_{\nu\nu}^j\right]$$
$$\nu^j(k\,|\,k-1) \equiv z(k) - H(k)\mu^j(k\,|\,k-1)$$
$$P_{\nu\nu}^j \equiv H(k)P_\mu^j(k\,|\,k-1)H(k)^{\mathrm{T}} + R(k)$$

Therefore, we have the filtered estimator

$$\hat{x}(k\,|\,k) = \sum_{j=1}^{m} \gamma^j(k\,|\,k)\mu^j(k\,|\,k) \tag{28}$$

The a priori density $p(x(k+1)\,|\,Z_k)$ can be rewritten with the same algorithm as the EKF as follows.

$$p(x(k+1)\,|\,Z_k) = \sum_{j=1}^{m} \gamma^j(k+1\,|\,k) \times N\left[\mu^j(k+1\,|\,k), P_\mu^j(k+1\,|\,k)\right] \tag{29}$$

where

$$\mu^j(k+1\,|\,k) = f(\mu^j(k\,|\,k)) \tag{30}$$

$$P_\mu^j(k+1\,|\,k) = F^j(k)P_\mu^j(k\,|\,k)F^{j\,\mathrm{T}}(k) + Q(k) \tag{31}$$

$$F^j(k) = \left[\frac{\partial f(x)}{\partial x}\right]_{x=\mu^j(k|k)} \tag{32}$$

$$\gamma^j(k+1\,|\,k) = \gamma^j(k\,|\,k)$$

4.2 Unscented Kalman filter

In the UKF, the predict mean $\hat{x}(k+1\,|\,k)$ and covariance $P(k+1\,|\,k)$ are calculated from a set of samples which is called the sigma points. This method is called the unscented transformation (Julier, 2000). Under the assumption that the system noise is independent and additive, the predict mean and covariance are computed as following steps.

Step1: choose the sigma points $\chi_j(k\,|\,k)$ which is associated with the n-dimensional state vector $x(k)$ as follows.

$$\chi_0(k\,|\,k) = \hat{x}(k\,|\,k), \quad W_0 = \frac{\kappa}{n+\kappa}$$
$$\chi_j(k\,|\,k) = \hat{x}(k\,|\,k) + \left(\sqrt{(n+\kappa)P(k\,|\,k)}\right)_j$$
$$\chi_{j+n}(k\,|\,k) = \hat{x}(k\,|\,k) - \left(\sqrt{(n+\kappa)P(k\,|\,k)}\right)_j$$
$$W_j = W_{j+n} = \frac{1}{2(n+\kappa)}, \qquad (j = 1, 2, \ldots, n)$$

Step2: compute a set of transformed samples through the process model equation (17),

$$\chi_j(k+1\,|\,k) = f(\chi_j(k\,|\,k), k)$$

Step3: compute the predicting mean and covariance as follows

$$\hat{x}(k+1\,|\,k) = \sum_{j=0}^{2n} W_j \chi_j(k+1\,|\,k)$$

$$P(k+1\,|\,k) = \sum_{j=0}^{2n} W_j \tilde{\chi}_j \tilde{\chi}_j^{\mathrm{T}} + Q(k)$$

where $\tilde{\chi}_j \equiv \chi_j(k+1\,|\,k) - \hat{x}(k+1\,|\,k)$

W_j is the weight of the *j*-th point and κ is a scaling parameter. $(\sqrt{(n+\kappa)P(k\,|\,k)})_j$ is the *j*-th column of the matrix square root of $(n+\kappa)P(k\,|\,k)$. Then, once the observation $z(k+1)$ is obtained, $\hat{x}(k+1\,|\,k)$ and $P(k+1\,|\,k)$ are updated to $\hat{x}(k+1\,|\,k+1)$ and $P(k+1\,|\,k+1)$ as follows.

$$Z_j(k+1\,|\,k) = H(k)\chi_j(k+1\,|\,k)$$

$$\hat{z}(k+1\,|\,k) = \sum_{j=0}^{2n} W_j Z_j(k+1\,|\,k) \tag{33}$$

$$P_{\nu\nu}(k+1\,|\,k) = \sum_{j=0}^{2n} W_j \tilde{Z}_j \tilde{Z}_j^{\mathrm{T}} + R(k) \tag{34}$$

$$P_{x\nu}(k+1\,|\,k) = \sum_{j=0}^{2n} W_j \tilde{\chi}_j \tilde{Z}_j^{\mathrm{T}} \tag{35}$$

where $\tilde{Z}_j \equiv Z_j(k+1\,|\,k) - \hat{z}(k+1\,|\,k)$

$$K(k+1) = P_{x\nu}(k+1\,|\,k)P_{\nu\nu}^{-1}(k+1\,|\,k) \tag{36}$$

$$\hat{x}(k+1\,|\,k+1) = \hat{x}(k+1\,|\,k) + K(k)(z(k) - \hat{z}(k+1\,|\,k)) \tag{37}$$

$$P(k+1\,|\,k+1) = P(k+1\,|\,k) - K(k)P_{\nu\nu}(k+1\,|\,k)K^{\mathrm{T}}(k) \tag{38}$$

Since the measurement equation (23) is linear in this navigation problem, above equations (33)-(35) can be simply expressed by

$$\hat{z}(k+1\,|\,k) = H(k)\hat{x}(k+1\,|\,k) \tag{39}$$

$$P_{\nu\nu}(k+1\,|\,k) = H(k)P(k+1\,|\,k)H^{\mathrm{T}}(k) + R \tag{40}$$

$$P_{x\nu}(k+1\,|\,k) = P(k+1 1k)H^{\mathrm{T}}(k) \tag{41}$$

4.3 Modified Gaussian Sum filter

In the Gaussian Sum filtering algorithm, we can see from equations (30)-(32) that the linearization technique is employed similarly to the extended Kalman filter. In this paper, we propose the modified Gaussian Sum filter by applying the unscented transformation algorithm to the time updating algorithm of the GSF, equations (30)-(32).

Step1: similarly to the step 1 of the UKF, for *j*-th ($j = 1, 2, \dots, N$) density in GSF, choose the sigma points and weights as follows.

$$\chi_0^j(k\,|\,k) = \mu^j(k\,|\,k), \quad W_0 = \frac{\kappa}{n+\kappa}$$

$$\chi_l^j(k\,|\,k) = \mu^j(k\,|\,k) + \left(\sqrt{(n+\kappa)P_\mu^j(k\,|\,k)}\right)_l$$

$$\chi_{l+n}^j(k\,|\,k) = \mu^j(k\,|\,k) - \left(\sqrt{(n+\kappa)P_\mu^j(k\,|\,k)}\right)_l$$

$$W_l = W_{l+n} = \frac{1}{2(n+\kappa)}, \qquad (l = 1, 2, \dots, n)$$

Step2: compute a set of transformed samples through the process model equation (17),

$$\chi_l^j(k+1\,|\,k) = f(\chi_l^j(k\,|\,k), k)$$

Step3: compute the *j*-th predicting mean and covariance as follows.

$$\mu^j(k+1\,|\,k) = \sum_{l=0}^{2n} W_l\, \chi_l^j(k+1\,|\,k) \tag{42}$$

$$P_\mu^j(k+1\,|\,k) = \sum_{l=0}^{2n} W_l\, \chi_l^j (\chi_l^j)^{\mathrm{T}} + Q(k) \tag{43}$$

$$\text{where} \quad \chi_l^j \equiv \chi_l^j(k+1\,|\,k) - \mu^j(k+1\,|\,k)$$

In the MGSF, the original time updating algorithm of equations (30) and (31) are substituted by (42) and (43) respectively.

5 Experimental results

The experiments of the INS/GPS In-Motion Alignment and navigation algorithms described above were carried out by using simulated INS and GPS data. In the experiments, we assume the vehicle runs at a speed of around 15 [km/h] for about 10 minutes. The speed at the start point was 0 [km/h], and the initial azimuth angle was 60 [deg]. The test trajectory in the local level horizontal plane is shown in Fig. 3. The data were obtained by utilizing the Matlab6.5 and INS Toolbox1.0 (GPSoft LLC.) at 50 [Hz] rate for IMU and at 1 [Hz] rate for GPS.

Four types of filters, i.e. EKF, GSF, UKF and MGSF are used in the experiments and compared. The nonlinearity of the INS usually occurs when there exist large attitude errors. So in the experiments, the initial state estimates are set to have large azimuth error. And we assume that there exist no errors in the other initial estimates. Therefore, in the EKF and UKF, the initial estimate $\hat{x}(0\,|-1)$ is set to 0, and $P(0\,|-1)$ and Q are configured from the nominal equipment specifications in Table 2. In this case, the states related to the azimuth error, i.e. 7th and 8th components of the state vector have 60 [deg] initial estimation error respectively.

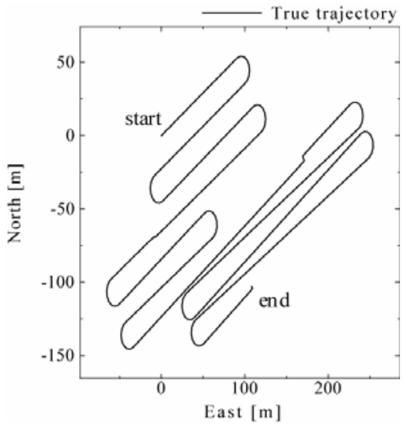

Fig. 3. Test trajectory

Table 2. Sensor error specification

Accelerometer	Specification	
Bias	80	[μ G] (1σ)
Scale factor	150	[ppm] (1σ)
Random error	0.0003	[m/s]^2

Gyroscope	Specification	
Bias	20	[deg/h] (1σ)
Scale factor	500	[ppm] (1σ)
Random error	0.06	[deg/ $\sqrt{h}$]

In the GSF and MGSF, three normal distributions are utilized, i.e. $m = 3$, and $P_\mu^j(0\,|-1)$, $j = 1, 2, 3$ are set to the same value of the EKF and UKF, i.e. $P_\mu^j(0\,|-1) = P(0\,|-1)$. The initial estimates $\mu^j(0\,|-1)$, $j = 1, 2, 3$ are also set to 0 except for the 7th and 8th components of the state vector (see Table), β and γ, that represent the azimuth error. They are assumed to have the initial azimuth error estimates such that $\delta\alpha = -60,\ 0,\ +60$ [deg].

The processing results are shown in Fig. (4)-(7). Figs. (4) and (5) show the results of the positioning and comparison of the positioning errors. Table 3 also shows RMS (Root Mean Square) values of the position errors. From Fig. (5) we can see that the MGSF shows faster convergence than the others, and the GSF and MGSF show better performances than EKF and UKF. Therefore, the GSF and MGSF can work well when there exist large azimuth error because they can treat large azimuth error by assuming multiple initial error distributions. From Table 3, we can also see that the MGSF achieves the best performance in this simulation.

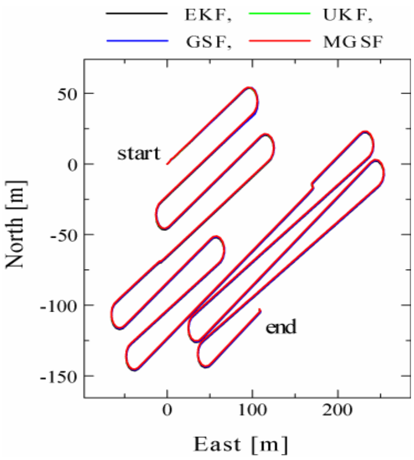

Fig. 4. Positioning results

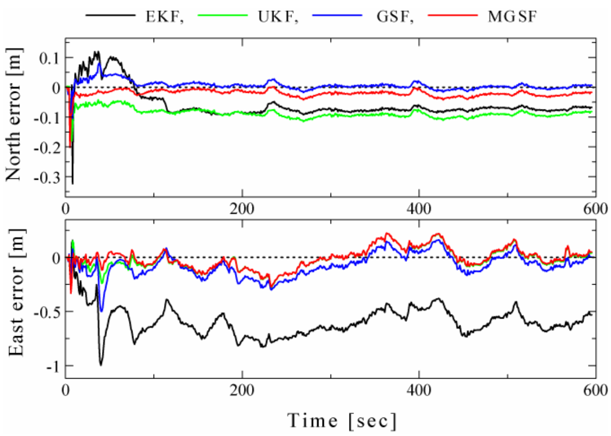

Fig. 5. Positioning errors

Table 3. Root mean square of position errors

	North error [m]	East error [m]
EKF	0.08	0.61
UKF	0.09	0.10
GSF	0.02	0.13
MGSF	0.02	0.09

Table 4. Root mean square of velocity errors

	North error [m/s]	East error [m/s]
EKF	0.36	0.25
UKF	0.34	0.19
GSF	0.36	0.22
MGSF	0.34	0.19

Fig. 6 and Table 4 show the velocity errors and their RMS values respectively. From these figures and tables, the all filters show almost same performance, whereas the UKF and MGSF show slightly better performance than the EKF and GSF.

Finally, Fig. 7 shows the results of the azimuth errors. From Fig. 7, we can see that all filters show almost same results after 200 [sec], but the MGSF shows faster convergence in its transient response from 0 to 200 [sec]. Therefore, from these results of the simulation, we can consider that the UKF and MGSF can achieve better performance than the EKF and GSF, and the MGSF can work well when there exist a large initial azimuth error.

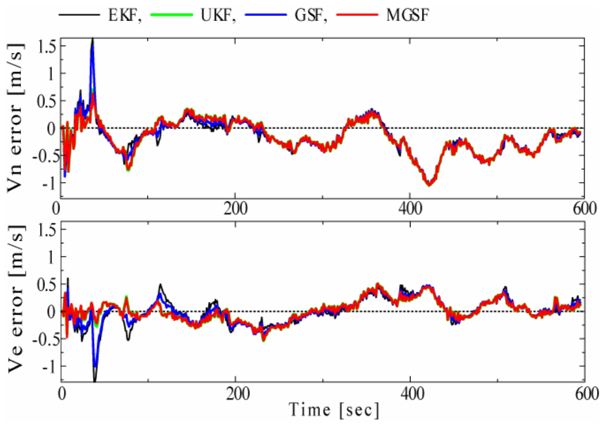

Fig. 6. Velocity errors

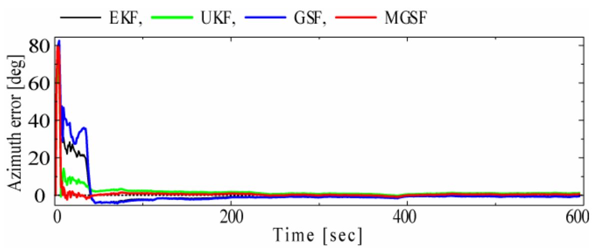

Fig. 7. Azimuth errors

6 Conclusions

In this paper, the modified Gaussian Sum filtering algorithm was derived by applying the unscented transformation to the Gaussian Sum filter, and it was applied to the GPS/INS integrated system. The algorithm was tested and compared with the EKF, GSF and UKF by using simulated data. From the experimental results, it was found that the derived MGSF show the quick transient response for azimuth error estimation. Therefore the MGSF has an ability to improve the navigation performance, when there are large initial azimuth errors.

References

Alspach D. L. and Sorenson H. W. (1972) ***Nonlinear Bayesian Estimation Using Gaussian Sum Approximations***, IEEE Trans. on Automatic Control, Vol. AC-17, No. 4, pp. 439-448, 1972.

An D. and Liccardo D. (2005) ***A UKF Based GPS/DR Positioning System for General Aviation***, Proc. of the Institute of Navigation, ION GNSS 2005, pp. 990-998, Long Beach, CA, 2005.

Doucet A., Godsill J. and Andrieu C. (2000) ***On sequential Monte Carlo sampling methods for Bayesian filtering***, Statistics and Computing, Vol. 3, pp. 197-208, 2000.

Fujioka S., Tanikawara M., Nishiyama M., Kubo Y. and Sugimoto S. (2005) ***Comparison of Nonlinear Filtering Methods for INS/GPS In-Motion Alignment***, Proc. of the Institute of Navigation, ION GNSS 2005, pp. 467-477, Long Beach, CA, 2005.

Gelb A. (1974) ***Applied Optimal Estimation***, MIT Press, Massachusetts, 1974.

Grewal M. S., Weill L. R. and Andrews A. P. (2001) ***Global Positioning Systems, Inertial Navigation, and Integration***, John Wiley & Sons, New York, 2001.

Julier S., Uhlmann J. and Durrant-Whyte H. F. (2000) ***A New Method for the Nonlinear Transformation of Means and Covariances in Filters and Estimators***, IEEE Trans. On Automatic Control, Vol. 45, No. 3, pp. 477-482, 2000.

Kitagawa G. (1996) ***Monte Carlo Filter and Smoother for Non-Gaussian Nonlinear State Space Models***, Jounal of Computational and Graphical Statistics, Vol. 5, pp. 1-25, 1996.

Maybeck P. S. (1979) ***Stochastic Models, Estimation and Control (Mathematics in Science and Engineering)***, Academic Press, New York, 1979.

Misra P. and Enge P. (2001) ***Global Positioning System -- Signals, Measurements, and Performance***, Ganga-Jamuna Press, Massachusetts, 2001.

Nishiyama M., Fujioka S., Kubo Y., Sato T. and Sugimoto S. (2006) ***Performance Studies of Nonlinear Filtering Methods in INS/GPS In-Motion Alignment***, Proc. of the Institute of Navigation, ION GNSS 2006, pp. 2733-2742, Fort Worth, TX, 2006.

Rogers R. M. (2001) ***Large Azimuth INS Error Models for In-Motion Alignment Land-Vehicle Positioning***, Proc. of the Institute of Navigation National Technical Meeting 2001, pp. 1104-1114, Long Beach, CA, 2001.

Rogers R. M. (2003) ***Applied Mathematics in Integrated Navigation Systems***, 2nd edition, AIAA, Virginia, 2003.

Shin E.-H. and El-Sheimy N. (2007) ***Unscented Kalman Filter and Attitude Errors of Low-Cost Inertial Navigation Systems***, Navigation: Journal of The Institute of Navigation, Vol. 54, No. 1, pp. 1-9, Spring, 2007.

Siouris G. M. (1993) ***Aerospace Avionics Systems A Modern Synthesis***, Academic Press, San Diego, 1993.

Sunahara Y. (1970) ***An Approximate Method of State Estimation for Nonlinear Dynamical Systems***, Journal of Basic Engineering, Trans. ASME, Series D, Vol. 92, No. 2, pp. 385-393, 1970.

Tanikawara M., Asaoka N., Oiwa M., Kubo Y. and Sugimoto S. (2004) ***Real-Time Nonlinear Filtering Methods for INS/DGPS In-Motion Alignment***, Proc. of the Institute of Navigation ION GNSS 2004, pp. 1104-1114, Long Beach, CA, 2004.

Yi Y. and Grejner-Brzezinka D. (2005) ***Nonlinear Bayesian Filter: Alternative To The Extended Kalman Filter In The GPS/INS Fusion Systems***, Proc. of the Institute of Navigation, ION GNSS 2005, pp. 1392-1400, Long Beach, CA, 2005.